VIP Imaging Agents

DOI: 10.1002/ange.201206939

Intrinsically Copper-64-Labeled Organic Nanoparticles as Radiotracers**

*Tracy W. Liu, Thomas D. MacDonald, Jiyun Shi, Brian C. Wilson, and Gang Zheng**

Nanotechnology has the potential to greatly expand the clinical armamentarium for diagnosing and treating disease. On the road to translating this promise into reality, "one of the top priorities is the determination of the distribution of nanoparticulate carriers in the body following systemic administration through any route".[1] Currently, the only technique that provides quantitative information about the whole body is radiolabeling, for which there are a number of approaches, as illustrated in Figure 1: A) the radionuclide is attached to the nanoparticle surface by an exogenous chelator; B) the radionuclide is entrapped in an enclosed compartment, or C) nanoparticles are manufactured from pre-radiolabeled building blocks. Each method suffers from some combination of the following limitations: in vivo instability and/or low specific activity (activity per unit mass) of the radiolabeled nanoparticle, or restrictive radiolabeling procedures with low radiochemical yields, long and complicated procedures, and narrow concentration ranges of the labeling.[1,2] Furthermore, the in vivo instability of exogenous chelators and entrapped radionuclides leads to concerns that the label is not faithful to the nanostructure or alters it such that the in vivo behavior of the radiolabeled nanoparticle differs from that of the same parent nanoparticles without the radiolabel.[1] By using prelabeled building blocks some of these concerns can be avoided, but the burden of manufacturing the nanoparticles is transferred to the end user. Therefore, the ideal approach would allow preformed nanoparticles to be labeled stably without affecting their in vivo behavior.

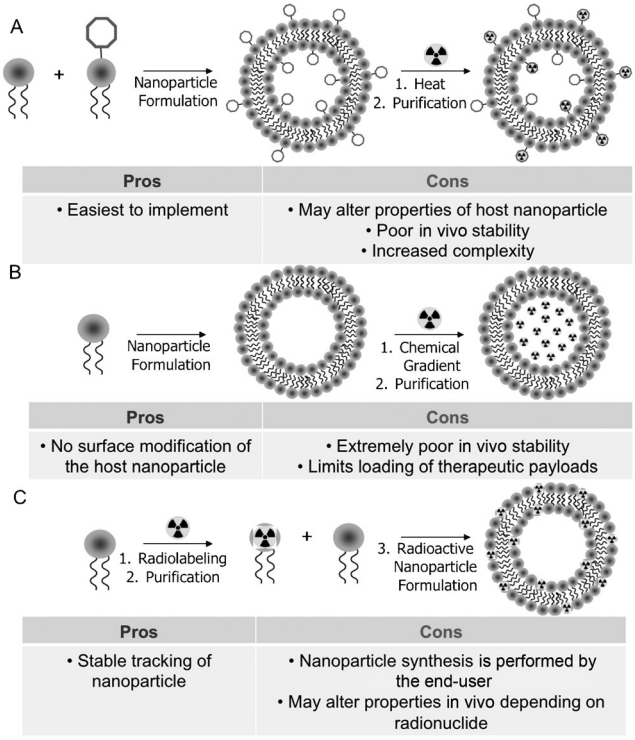

Figure 1. Established strategies for the radiolabeling of nanoparticles. A) Incorporation of an exogenous chelator into the nanoparticle formulation and subsequent radiolabeling. B) Entrapping the radiolabel into an enclosed compartment within the nanoparticle. C) Radiolabeling of building blocks with subsequent formulation and synthesis of the nanoparticle.

Herein, we introduce a novel, exogenous-chelator-free nanoplatform that has intrinsic capacity for use as a radiotracer and for which the sole modification is the inclusion of a radionuclide directly into the building blocks of the preformed nanoparticles. This strategy takes advantage of the unique properties of porphysomes, which are completely organic, nontoxic, biodegradable nanovesicles formed from aqueous self-assembly of porphyrin–lipid conjugates into liposome-like bilayers.[3] Porphysomes possess all the functionality of liposomes, such as drug-delivery capabilities and an easily functionalized surface, while also exhibiting strong photonic properties.[3] All of these unique properties are derived from a single building block, porphyrin–lipid conjugate. Here, we extend the capability of porphysomes by

[*] T. W. Liu,[+] T. D. MacDonald,[+] Prof.Dr. B. C. Wilson, Prof.Dr. G. Zheng
Ontario Cancer Institute, Campbell Family Institute for Cancer Research and Techna Institute, UHN (Canada)
E-mail: gang.zheng@uhnres.utoronto.ca
T. W. Liu,[+] Dr. J. Shi, Prof.Dr. B. C. Wilson, Prof.Dr. G. Zheng
Department of Medical Biophysics, University of Toronto (Canada)
T. D. MacDonald,[+] Prof.Dr. G. Zheng
Department of Pharmaceutical Sciences
University of Toronto (Canada)
Dr. J. Shi
Medical Isotopes Research Center, Peking University
Beijing (China)
[+] These authors contributed equally to this work.

[**] We would like to thank Dr. Warren Foltz for assistance with MR imaging, Tab Siddiqi and Dr. David Green for assistance with the radioUPLC, Dr. Helen Lee, Dr. Jinzi Zhang, and Dr. Wing-Ki Liu for assistance with the pharmacokinetics study, Cheng S. Jin for assistance with the orthotopic prostate cancer model, Dr. David Jaffray and the staff of the STTARR facility for assisting with obtaining ^{64}Cu, and Todd Cunningham for illustrating Figure 2A. Funding was provided by CIHR, OICR, SERC, CFI, the Princess Margaret Cancer Foundation, MaRS Innovation, Joey and Toby Tanenbaum/Brazilian Ball Chair in Prostate Cancer Research, and the US Army BCRP Predoctoral Award W81XWH-10-1-0115.
Supporting information for this article is available on the WWW under http://dx.doi.org/10.1002/anie.201206939.

exploiting the natural ability of the porphyrin–lipid conjugates to form stable, high-affinity complexes with copper-64 (^{64}Cu),[4] which has favorable characteristics for nanoparticle tracking through positron emission tomography (PET): $t_{1/2}$ = 12.7 h, β^+: 17.4%, $E_{\beta+max}$ = 656 keV.[5] Importantly, it was demonstrated in the 1980s that the in vivo pharmacokinetics and biodistribution of porphyrins are not altered by chelation with ^{64}Cu[4a–c] because the Cu atom fits into the center of the tetrapyrrole ring without altering the side chains that determine the in vivo behavior. We take advantage of porphyrins' intrinsic ability to chelate metals to incorporate the radionuclide into the nanoparticle. This approach allows for the direct radiolabeling of preformed porphysomes with ^{64}Cu without altering their behavior in vivo, and yields highly stable radiolabeled photonic nanoparticles. By using a simple, stable, and robust direct radiolabeling strategy, we increase the functionality of an organic nanoparticle and then we demonstrate its novel use as a tumor imaging agent in a primary (orthotopic) prostate cancer model.

An effective radiolabeling procedure should be fast and efficient, and yield a radiotracer that requires minimal purification, has impeccable stability, and an in vivo half-life that is commensurate with the radionuclide half-life. Our radiolabeling strategy fulfills all of these requirements. The direct ^{64}Cu labeling of porphysomes is a fast and simple one-pot procedure (Figure 2A): a solution of preformed porphysomes (1 mM porphyrin–lipid building block) in 0.1M NH_4OAc buffer (pH 5.5) is mixed with aqueous $^{64}CuX_2$ (2.5 mCi μmol^{-1} porphyrin–lipid building block; X = OAc, Cl) and heated to 60°C for 30 min. The reaction yields ^{64}Cu-porphysomes with radiochemical purities of greater than 98% in decay-uncorrected radiochemical yields of greater than 95%, as determined by radio-UPLC (ultra performance liquid chromatography) and size-exclusion centrifugation filtration (Figure 2B). The procedure attaches a ^{64}Cu label to less than 5% of the porphyrin moieties in the porphysomes, and leaves the nanoparticle size and photonic properties unaffected (see the Supporting Information, Figure S1).

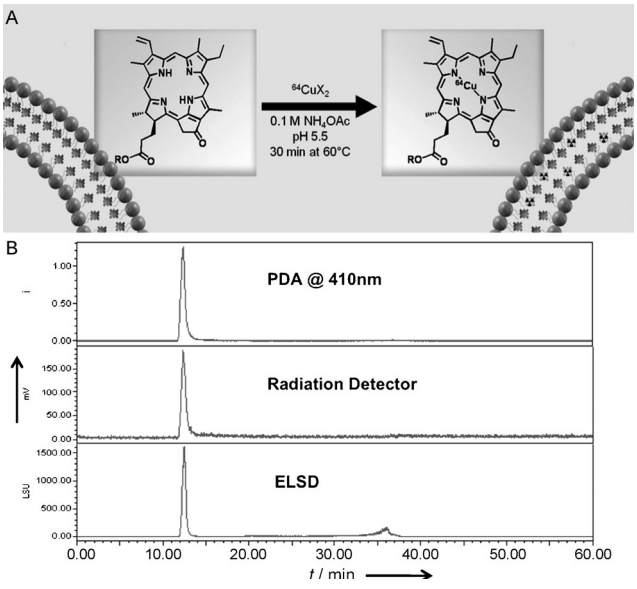

Figure 2. A) Direct radiolabeling of preformed porphysomes. B) Quality control of ^{64}Cu-porphysomes using radio-UPLC (the smaller peak is cold buffer salts). ELSD = evaporation light-scattering detection, PDA = photodiode array detector.

Having attained nearly ideal radiolabeling under our initial conditions, we sought to test the robustness and flexibility of the procedure. When we varied the concentration of porphysomes over four serial dilutions (4 μM to 4 mM, at 2.5 mCi μmol^{-1}) we found that labeling proceeded with over 95% radiochemical purity (RCP) for concentrations between 40 μM and 4 mM (Figure 3A). The radiolabeling is

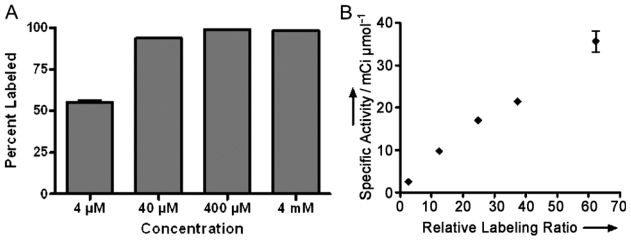

Figure 3. A) ^{64}Cu-labeling efficiency across four serial dilutions (n = 3). B) Specific activity per porphyrin–lipid molecule for a variety of $^{64}CuX_2$ to porphyrin-lipid building block ratios (n = 3). Mean ± 1 standard deviation.

effective over a 100-fold concentration range, a robustness rarely achieved using other nanoparticle radiolabeling strategies. To test the flexibility of the system, we determined the range of specific activities accessible by varying the ratio of $^{64}CuX_2$ to porphyrin–lipid conjugate (Figure 3B). Specific activities up to 36 mCi μmol^{-1} of the porphyrin–lipid conjugate were attained, this corresponds to a specific activity of 2800 Ci μmol^{-1} per nanoparticle, the highest activity ever reported for a ^{64}Cu-labeled nanoparticle.[2i] The speed, flexibility, and robustness of the approach make ^{64}Cu-porphysomes attractive for a number of applications. The ability to "pull them off the shelf", radiolabel, and then use them make ^{64}Cu-porphysomes good candidates to become PET radiotracers. Additionally, because of the unique decay properties of ^{64}Cu, ^{64}Cu-porphysomes could be used as a radiotherapeutic.

With these promising potential applications of ^{64}Cu-porphysomes in mind, we confirmed in vivo that ^{64}Cu was a suitable radioisotope for porphysomes. The concentration of radioactivity in blood plasma over time was found to fit a two-compartment model, $C(t) = 28.01\,e^{(-0.56t)} + 33.62\,e^{(-0.062t)}$ with a log plot of $r^2 > 0.95$, and with short and long half-lives of 1.23 and 11.1 h (Figure 4A). Therefore, ^{64}Cu is well-suited as a porphysome radiotracer, as its physical half-life (12.7 h) closely matches the long biological half-life of porphysomes (11.1 h). The portion of the total radioactivity caused by the ^{64}Cu-porphysomes bound to the blood cells was significant immediately after the intravenous injection (19.5%) but decreased to < 5% after 4 h (Figure S2). The stability of ^{64}Cu chelation to porphysomes was 99.3 ± 0.6% and 98.6 ± 0.9% after 24 and 48 h in 50% FBS, respectively, thus demonstrating the high affinity of ^{64}Cu for the porphyrin chelator

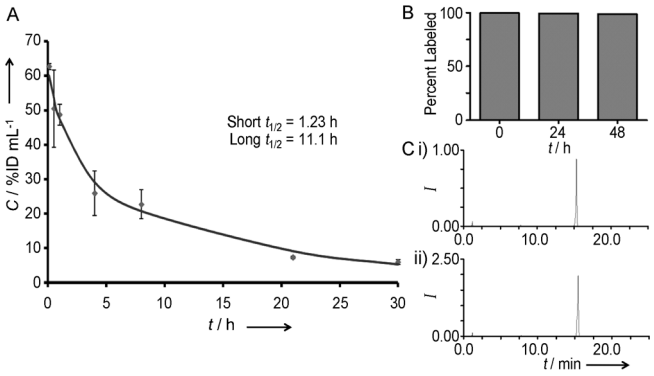

Figure 4. A) Blood clearance curve after intravenous injection of ^{64}Cu-porphysomes in healthy male mice. ◆ experimental data; —— two-compartment model; $n=3$; error bars represent ± 1 standard deviation on the mean). B) ^{64}Cu chelation stability in serum (50% FBS) for 24 h and 48 h ($n=3$). C) Representative HPLC traces illustrating monomer chemical integrity in vivo i) 4 h and ii) 30 h after the intravenous injection ($n=3$). ID = injected dose.

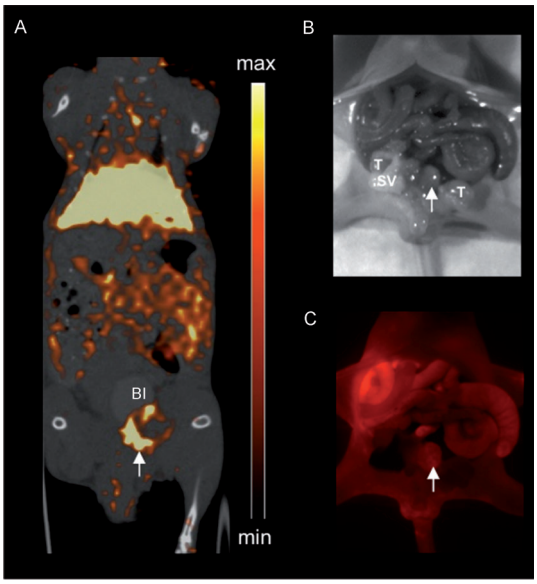

Figure 5. In vivo multimodal imaging of ^{64}Cu-porphysomes in orthotopic prostate cancer model. A) Representative MicroPET/CT images of coronal single slices through orthotopic PC3 tumor ($n=4$) at 24 h after intravenous injection of 500 μCi ^{64}Cu-porphysomes. PET image integration time 40 min. B) White light image of orthotopic PC3 prostate tumor model. C) Fluorescent image of orthotopic PC3 prostate tumor model. White arrows indicate prostate tumor, Bl indicates the bladder; SV indicates the seminal vesicles, and T indicates the testes.

(Figure 4B). The porphyrin–lipid ^{64}Cu-porphysome was chemically stable in the circulation for at least 30 h (Figure 4C), thus indicating that in vivo (e.g. PET imaging) measurements describe accurately the behavior of the ^{64}Cu-porphysomes and not that of a cleaved chelator. The closely matched biological half-life of porphysomes (11.1 h) and the physical half-life of ^{64}Cu (12.7 h), and the fidelity of the radionuclide to the nanoparticle reinforce the rationale of pairing ^{64}Cu with porphysomes.

Direct labeling of the building blocks, as achieved here, is the most reliable and accurate method for quantitatively tracking the distribution of nanoparticles in vivo. We selected prostate cancer as the platform on which to evaluate ^{64}Cu-porphysomes. Prostate tumors are on average twice as vascularized as most of the surrounding healthy prostate tissue.[6] Thus, they are amenable to treatment with ^{64}Cu-porphysomes, relying on the tumor's vasculature, which is characterized by irregular and leaky blood vessels, to enhance delivery, uptake, and retention in the malignant tissue.[7] We used an orthotopic PC3 prostate cancer model to best mimic localized primary cancer. The tumor uptake of the ^{64}Cu-porphysomes was evaluated at 24 h post injection by PET/CT (Figure 5A) and fluorescence imaging (Figure 5B and C). The PC3 tumors were clearly delineated in both imaging modalities with very little local background. It should be noted that the intensity of porphysome fluorescence is dependent upon the nanoparticle dissociation, which may not be complete at 24 h. Further in vivo work is currently being pursued. Similar to many other nanoparticles, porphysomes are cleared through the hepatobilliary route, thus resulting in high accumulation within the liver and spleen and little to none in the bladder. This property is important as high bladder accumulation obscures the prostate, which has been the "Achilles heel" of many small molecule radiotracers.

The incorporation of PET properties into optical probes addresses many limitations currently faced by each of these imaging techniques. PET provides noninvasive imaging of the whole body with deep tissue penetration and quantitative nanoparticle distribution[8] that is not achievable by fluorescence. Conversely, fluorescence can be used for real-time, high resolution imaging of accessible tissues.[9] For example, PET imaging of ^{64}Cu-porphysomes would enable pretreatment planning for fluorescence-image-guided prostatectomy. The fraction of ^{64}Cu labeling of the porphyrin building blocks can be fine-tuned to the specific imaging application. A highly-labeled formulation would be best suited for image-tracked radiotherapy, whereas low or intermediate fractional labeling would allow the full exploitation of porphysomes' multimodal nature. The porphyrin–lipid building blocks of porphysomes can be tailor-made with a range of porphyrinoids, such as bacteriochlorins[3,10] or texaphyrins, to chelate a variety of radionuclides, such as cobalt-60 or lutetium-177. However, the procedure may need to be optimized based on the chemistry of the porphynoid and radionuclide pairing.

The incorporation of labels for PET imaging into a multifunctional nanoparticle through a fast (30 min), one-pot, high yielding (> 95%) procedure produces a highly stable radiolabeled nanoparticle that can achieve the highest specific activity ever reported for a nanoparticle labeled with ^{64}Cu. It is the intrinsic ability of the preformed porphysomes to directly chelate ^{64}Cu that allows them to be accurately and noninvasively tracked in vivo. However it is the fast, flexible, and robust radiochemistry that provides ^{64}Cu–porphysomes with a range of promising clinical applications. The speed, ease, and stability of the labeling lend this method to creating a dual-mode PET/fluorescence imaging probe that could potentially be used in radiotherapy. Importantly, the flexibility of the labeling gives the freedom to tailor the extent of

labeling to the application. In vivo, ^{64}Cu-porphysomes can clearly delineate diseased tissue in a clinically relevant orthotopic prostate cancer model, thus showing great promise for translation of this approach to clinical applications. The realization of this potential will ultimately rely on the highly efficient, robust, and flexible radiochemistry presented here.

Received: August 27, 2012
Published online: November 14, 2012

Keywords: fluorescence · porphyrins · positron emission tomography · prostate cancer · radiochemistry

[1] W. R. Sanhai, J. H. Sakamoto, R. Canady, M. Ferrari, *Nat. Nanotechnol.* **2008**, *3*, 242 – 244.
[2] a) A. Louie, *Chem. Rev.* **2010**, *110*, 3146 – 3195; b) W. T. Phillips, B. A. Goins, A. Bao, *Wiley Interdiscip. Rev. Nanomed. Nanobiotechnol.* **2009**, *1*, 69 – 83; c) C. A. Boswell, X. Sun, W. Niu, G. R. Weisman, E. H. Wong, A. L. Rheingold, C. J. Anderson, *J. Med. Chem.* **2004**, *47*, 1465 – 1474; d) C. L. Ferreira, D. T. Yapp, S. Crisp, B. W. Sutherland, S. S. Ng, M. Gleave, C. Bensimon, P. Jurek, G. E. Kiefer, *Eur. J. Nucl. Med. Mol. Imaging* **2010**, *37*, 2117 – 2126; e) J. W. Seo, H. Zhang, D. L. Kukis, C. F. Meares, K. W. Ferrara, *Bioconjugate Chem.* **2008**, *19*, 2577 – 2584; f) J. Marik, M. S. Tartis, H. Zhang, J. Y. Fung, A. Kheirolomoom, J. L. Sutcliffe, K. W. Ferrara, *Nucl. Med. Biol.* **2007**, *34*, 165 – 171; g) A. L. Petersen, T. Binderup, P. Rasmussen, J. R. Henriksen, D. R. Elema, A. Kjaer, T. L. Andresen, *Biomaterials* **2011**, *32*, 2334 – 2341; h) S. Li, B. Goins, W. T. Phillips, A. Bao, *J. Liposome Res.* **2011**, *21*, 17 – 27; i) D. Zeng, N. S. Lee, Y. Liu, D. Zhou, C. S. Dence, K. L. Wooley, J. A. Katzenellenbogen, M. J. Welch, *ACS Nano* **2012**, *6*, 5209 – 5219.
[3] J. F. Lovell, C. S. Jin, E. Huynh, H. Jin, C. Kim, J. L. Rubinstein, W. C. Chan, W. Cao, L. V. Wang, G. Zheng, *Nat. Mater.* **2011**, *10*, 324 – 332.
[4] a) R. Bases, S. S. Brodie, S. Rubenfeld, *Cancer* **1958**, *11*, 259 – 263; b) W. P. Jeeves, B. C. Wilson, G. Firnau, K. Brown, *Adv. Exp. Med. Biol.* **1985**, *193*, 51 – 67; c) B. C. Wilson, G. Firnau, W. P. Jeeves, K. L. Brown, D. M. Burns-McCormick, *Laser Med. Sci.* **1988**, *3*, 71 – 80; d) J. Shi, T. W. Liu, J. Chen, D. Green, D. Jaffray, B. C. Wilson, F. Wang, G. Zheng, *Theranostics* **2011**, *1*, 363 – 370.
[5] P. J. Blower, J. S. Lewis, J. Zweit, *Nucl. Med. Biol.* **1996**, *23*, 957 – 980.
[6] S. A. Bigler, R. E. Deering, M. K. Brawer, *Hum. Pathol.* **1993**, *24*, 220 – 226.
[7] Y. Matsumura, H. Maeda, *Cancer Res.* **1986**, *46*, 6387 – 6392.
[8] S. S. Gambhir, *Nat. Rev. Cancer* **2002**, *2*, 683 – 693.
[9] R. Weissleder, M. J. Pittet, *Nature* **2008**, *452*, 580 – 589.
[10] T. W. Liu, J. Chen, L. Burgess, W. Cao, J. Shi, B. C. Wilson, G. Zheng, *Theranostics* **2011**, *1*, 354 – 362.
[11] J. F. Lovell, C. S. Jin, E. Huynh, T. D. Macdonald, W. Cao, G. Zheng, *Angew. Chem.* **2012**, *124*, 2479 – 2483; *Angew. Chem. Int. Ed.* **2012**, *51*, 2429 – 2433.